Development/Plasticity/Repair

Gap Junctions Modulate Interkinetic Nuclear Movement in Retinal Progenitor Cells

Rachael A. Pearson,[1] Nanna L. Lüneborg,[1] David L. Becker,[2] and Peter Mobbs[1]
Departments of [1]Physiology and [2]Anatomy and Developmental Biology, University College London, London WC1E 6BT, United Kingdom

During early retinal development, progenitor cells must divide repeatedly to expand the progenitor pool. During G_1 and G_2 of the cell cycle, progenitor cell nuclei migrate back-and-forth across the proliferative zone in a process termed interkinetic nuclear movement. Because division can only occur at the ventricular surface, factors that affect the speed of nuclear movement could modulate the duration of the cell cycle. Gap-junctional coupling and gap junction-dependent Ca^{2+} activity are common features of proliferating cells in the immature nervous system. Furthermore, both gap-junctional coupling and changes in $[Ca^{2+}]_i$ have been shown to be positively correlated with the migration of a number of immature cell types. Using time-lapse confocal microscopy, we describe the nature and rate of progenitor cell interkinetic nuclear movement. We show that nuclear movement is usually, but not always, associated with Ca^{2+} transients and that buffering of these transients with BAPTA slows movement. Furthermore, we show for the first time that gap-junctional communication is an important requirement for the maintenance of normal nuclear movement in retinal progenitor cells. Conventional blockers of gap junctions and transfection of cells with dominant-negative constructs of connexin 43 (Cx43) and Cx43-specific antisense oligodeoxynucleotides (asODNs) all act to slow interkinetic nuclear movement. The gap junction mimetic peptide Gap26 also acts to slow movement, an effect that we show may be attributable to the blockade of gap junction hemichannels.

Key words: **Ca^{2+} waves; chick; hemichannel; proliferation; connexin43; antisense**

Introduction

The vertebrate eye originates from the optic cup; the outer layer forms the retinal pigment epithelium (RPE), whereas the inner layer divides repeatedly to produce the neurons and glia of the neural retina. The mature chick retina consists of approximately two hundred million cells, most of which are produced during the first week of development. A complex array of intrinsic and extrinsic control mechanisms are required to ensure that these cells are produced at the right time, in the correct numbers, and adopt the correct fate. Within the immature neural retina, mitosis is confined to a region immediately adjacent to the RPE, the ventricular zone (Robinson et al., 1985). Progenitor cell nuclei undergo interkinetic nuclear movement, moving from the ventricular zone to the vitreal surface in G_1 of the cell cycle, before replicating their DNA in S-phase, returning to the ventricular zone in G_2 and undergoing mitosis (supplemental Fig. 1, available at www.jneurosci.org as supplemental material). After terminal division, postmitotic cells (G_0) migrate from the ventricular zone to locations appropriate to their fate. Because mitosis can only occur within the ventricular zone, factors affecting the rate of interkinetic nuclear movement may influence the duration of the cell cycle and, consequently, proliferation. Despite these implications, research on cell movements in development, and the factors that may modulate them, has focused on the migration of postmitotic neurons rather than the nuclear movements of progenitor cells.

Gap-junctional communication, via intercellular gap junction channels, is a prominent feature of the developing CNS. In both the embryonic retina and cortex, gap junction channels couple progenitor cells into extensive networks that primarily exclude differentiated neurons (LoTurco and Kriegstein, 1991; Bittman et al., 1997; Owens and Kriegstein, 1998; Pearson et al., 2004). Coupling between proliferating progenitor cells is strong (Bittman et al., 1997; Pearson et al., 2004) but is attenuated during terminal differentiation (Bittman et al., 1997; Tamalu et al., 2001). We have shown previously that gap-junctional coupling is positively correlated with cell proliferation: suppressing expression of connexin 43 (Cx43), the first gap junction protein expressed in the embryonic chick eye (Becker et al., 2002), impedes progenitor proliferation and results in small eyes (Becker and Mobbs, 1999). In other immature cell types, such as neural crest cells, the extent of gap-junctional coupling is positively correlated with the rate of cell migration (Ewart et al., 1997; Huang et al., 1998; Bannerman et al., 2000). Together, these observations raise the possibility that gap junctions could influence proliferation via actions on progenitor cell interkinetic nuclear movement.

It is not yet known how gap-junctional communication might regulate interkinetic nuclear movement. However, coupling permits the passage of signaling molecules, such as Ca^{2+}, between adjacent cells. Gap junction-dependent Ca^{2+} activity is widespread in the immature CNS, and changes in $[Ca^{2+}]_i$ play pivotal

Received Feb. 1, 2005; revised Oct. 3, 2005; accepted Oct. 5, 2005.

This work was supported by the Wellcome Trust. We thank David Attwell for his helpful comments on this manuscript and Daniel Ciantar for technical assistance with confocal microscopy.

*R.A.P. and N.L.L. contributed equally to this work.

Correspondence should be addressed to Dr. Rachael Pearson at her present address: Developmental Biology Unit, Institute of Child Health, University College London, 30 Guilford Street, London WC1N 1EH, UK. E-mail: rachael.pearson@ich.ucl.ac.uk.

DOI:10.1523/JNEUROSCI.2312-05.2005

 0270-6474/05/2510803-12$15.00/0

roles in the regulation of both cell movement and proliferation. For example, the saltatory movements of migratory neurons require Ca^{2+} transients, and the speed of movement is positively correlated with both the frequency and amplitude of Ca^{2+} changes (Komuro and Rakic, 1996, 1998). Cortical radial glia, which function as progenitor cells in development (Noctor et al., 2002), undergo spontaneous Ca^{2+} waves, and disruption of the waves decreases proliferation (Weissman et al., 2004). Because gap junction-mediated Ca^{2+} wave activity also occurs among retinal progenitor cells (Pearson et al., 2002, 2004), we considered the hypothesis that, in the retina, gap-junctional communication might exert its effects on proliferation via actions on interkinetic nuclear movement. We describe the relationship between Ca^{2+} signaling, cell movement, and gap-junctional communication and show that gap junction function is necessary for the maintenance of the normal rate of progenitor cell interkinetic nuclear movement.

Materials and Methods

Retinal preparations

Embryonic day 5 (E5) White Leghorn or Rhode Island Red chicken embryos were decapitated, and the eyes were removed and dissected from the overlying sclera at room temperature (RT) in Krebs' solution containing the following (in mM): 100 NaCl, 30 $NaHCO_3$, 6 KCl, 3 NaH_2PO_4, 1 $MgCl_2$, 1 $CaCl_2$, and 20 glucose (pH7.4 by gassing with 5% CO_2/95% O_2).

Cell movement

The vital dye DiI was used to follow the movement of cells; it is incorporated irreversibly into the plasma membrane of cells that contact the dye but does not spread from labeled to unlabeled cells (Honig and Hume, 1986; Lumsden et al., 1991). Cells were labeled using one of two methods: the biolistic technique described by Gan et al. (2000) or by bath immersion of retinal preparations in Krebs' solution containing DiI. The rates of movement were the same for both methods.

Biolistic labeling

Membrane dyes. A solution of DiI (Invitrogen, Paisley, UK) was prepared (1 mg/200 μl dichloromethane; Sigma, Poole, UK). A total of 40 mg of tungsten particles (1 μm diameter; Bio-Rad, Hemel Hempstead, UK) were mixed with dye solution and spread onto a glass slide. Particles were left until completely dry (~20 min) before being removed by scraping the slide with a razor blade and poured into ~25 cm length of Bio-Rad Goldcoat plastic tubing precoated with polyvinylpyrrolidine (100 mg/ml in ethanol; Sigma) and distributed by gentle shaking. The tubing was dried using N_2, cut into appropriate lengths (13 mm), and stored in the dark at 4°C.

Calcium indicators. A total of 1–2 mg of calcium indicator [Oregon Green 488 BAPTA-1, conjugated to dextran, 10,000 kDa molecular weight (MW); Invitrogen] was dissolved in 50 μl of distilled water and thoroughly mixed with 40 mg of tungsten particles. The indicator-coated particles were then dried, loaded, and stored, as described above.

Particle delivery. Retinas were either mounted on Millipore (Watford, UK) inserts (see below) or flattened, ventricular surface uppermost, on a slide, and any excess solution was removed. Particles were delivered using a Helios gene gun (Bio-Rad), fired at ~60 psi (helium gas). A track-etched membrane filter (cell culture inserts with 3 μm pore size, 8.0×10^5 pores/cm^2, Falcon; Becton Dickinson, Mountain View, CA) was inserted between the gun and each preparation to prevent large clusters of particles from landing on the tissue and reduce the shock wave generated by the gene gun.

Immersion labeling

Retinas were incubated for 10 min at 36°C in 2 ml of Krebs' solution containing 1 μl of DiI solution (50 μg of DiI/50 μl of DMSO). DiI is highly hydrophobic, dissolving readily in the solvent DMSO. When added to Krebs' solution, the dye solution forms a sparse suspension of droplets that settle on the surface of the tissue, labeling the cells beneath.

Modulating gap-junction function

In addition to pharmacological blockers, gap-junction function was manipulated using one of two techniques: transfection of individual cells with wild-type or dominant-negative constructs of Cx43 (dnCx43) or by gel application of Cx43-specific antisense oligodeoxynucleotides.

Phosphorylated internal ribosomal entry site 2–enhanced green fluorescent protein constructs

Retinas were mounted onto 13-mm-diameter Millipore nitrocellulose filters, ventricular zone uppermost. Filters were placed on a coiled platinum wire electrode, and a small amount of construct (2 μl; 1 μg/μl) was placed on the ventricular surface of the retina. A second platinum electrode was brought close enough to form a meniscus with the vector-containing solution but not so close as to touch the tissue. Current pulses, 50 ms/50 V, were applied at a frequency of 100 Hz as the electrode was moved laterally over the surface of the retina. This process was performed swiftly to avoid the retina drying out. Three enhanced green fluorescent protein (eGFP) phosphorylated internal ribosomal entry site 2 (pIRES2) vectors were used: dnCx43, wild-type Cx43, or eGFP alone (Becker et al., 2001). After electroporation, retinas were placed in DMEM containing 10% fetal calf serum, 4 mM L-glutamine, and 100× penicillin–streptomycin (1 ml/100 ml) (all from Sigma) and incubated at 36°C overnight. Preparations were viewed using a fluorescence dissection microscope (FLIII; Leica, Milton Keynes, UK) to check for the extent of GFP labeling.

Cx43 asODNs

Pluronic F-127 gel (30% in PBS; BASF/Knoll, Ludwigshafen, Germany) was used to deliver Cx43-specific unmodified antisense ODNs (Sigma-Genosys, Haverhill, UK) at a concentration of 1 μM. This gel is liquid between 0 and 4°C but sets in place at room temperature. The gel is also a mild surfactant and thus expedites ODN penetration into cells. Retinas were mounted on Millipore nitrocellulose filters before gel application, before being transferred to culture wells containing DMEM and incubated at 36°C, before labeling. Knockdown was rapid, with Cx43 protein expression reduced by 95% after a 2 h exposure to asODN compared with gel-only controls. Counts of the number of Cx43 plaques and of pixel number were used to determine the extent of Cx43 knockdown after antisense treatment. The number of Cx43 plaques was reduced from 2527 ± 290 plaques in sense controls to 154 ± 46 after treatment with antisense ODNs. Similarly, the total pixel count was reduced from 7286 ± 991 pixels/25×10^3 μm^2 in sense controls to 200 ± 115 in antisense ODN-treated preparations. Additional details of antisense characterization have been described previously by Becker et al. (1999). After 4 h incubation, retinas were labeled with DiI (Invitrogen) as described above. Retinas were fixed and processed in parallel for Cx43 immunostaining both before and after imaging to monitor the extent of Cx43 knockdown (see Fig. 5*G*). Staining for Cx43 was performed following a protocol adapted from Becker et al. (1995). Briefly, retinas were fixed in 4% paraformaldehyde (PFA) (made in PBS) before permeabilization and exposure to primary antibodies against Cx43/Gap1A (mouse monoclonal, 1:100) (Wright et al., 2001). The primary antibody was labeled using Alexa 488-tagged secondary antibody.

Assessing and modulating hemichannel function

Gap-junction hemichannel (unopposed gap-junction connexons) function was manipulated using the connexin mimetic peptide Gap26 (VCYDKSFPISHVR) (Braet et al., 2003; Pearson et al., 2005). A scrambled version of the Gap26 peptide (PSFDSRHCIVKYV) served as a control.

Dye fills

Dye diffusion between cells was used to confirm the specificity of Gap26 for hemichannels as opposed to an effect on whole gap junctions (Braet et al., 2003; Pearson et al., 2005). Neural retinal progenitor cells were filled using the methods described by Pearson et al. (2004). Briefly, patch pipettes were filled with 1% FITC–dextran (10,000 kDa MW)/1% Neurobiotin (323 kDa MW) in an internal solution containing the following (in

mm): 103 Cs-gluconate, 2 $MgCl_2$, 0.1 $CaCl_2$, 40 HEPES, 5 *N*-methyl-D-glucamine–EGTA, and 1 Na_2ATP, pH 7.35 with CsOH. High-resistance seals (>1 GΩ) were made on cell bodies or processes, and cells were kept in whole-cell mode for 2 min before withdrawing the pipette. Done carefully, the membrane sealed over and the dyes were left trapped within the cell. Retinas were left for 30 min to allow time for the Neurobiotin to diffuse into any cells coupled to the injected cell (Catsicas et al., 1998; Pearson et al., 2004). Dye fills were made in control solution, carbenoxolone (CBX) (100 μM), or after incubation (2 h, the same duration as used in the migration experiments) with either Gap26 (25 mg/ml) or scrambled Gap26 (25 mg/ml).

Neurobiotin histochemistry. Retinas were fixed in 4% PFA in PBS at 4°C, rinsed three times for 10 min in PBS, and blocked/permeabilized in 0.1% Triton X-100 (Sigma) and 0.1 M L-lysine (Sigma) in PBS for 4 h at RT. The tissue was then washed free of this solution with PBS (three times for 30 min) and incubated in 1:100 cyanine 3 (Cy3)–streptavidin (Invitrogen) for 12 h at 4°C. Unbound Cy3 was removed by washing in PBS for three times for 30 min, and the retinas were mounted in Citifluor (Citifluor, London, UK) under thin glass coverslips.

Hemichannel histochemistry

An antibody, Gap7M, raised to a region on the external loop of Cx43 that is occluded in complete gap junctions (Becker et al., 1995), was used to examine the distribution of gap-junction hemichannels in the retina. Chick embryo heads were fixed in 4% PFA/PBS for 2 h, transferred to 20% sucrose/PBS overnight at 4°C, embedded in OTC (Tissue-Tek; Miles, Cambridge, UK), and frozen. Cryostat sections (20 μm thick) were cut and affixed to poly-L-lysine-coated slides. Sections passing through the center of the retina adjacent to the optic nerve were processed. Blocking solution containing polyclonal rabbit anti-Gap7M primary antibody (1:100) was applied for 4 h at RT. After rinsing three times for 10 min with PBS, the sections were incubated with an anti-rabbit Alexa 488-tagged secondary antibody (1:500; Invitrogen) for 4 h at RT. After an additional three times for 10 min rinse with PBS containing 2 μM Hoechst 33342, sections were mounted in Citifluor (Citifluor) underneath a coverslip. Negative controls consisted of retinas processed as above but in the absence of primary antibody.

Confocal imaging

Labeled retinal whole mounts were transferred to a gas-, humidity-, and temperature- (5% CO_2, 100% relative humidity, 36°C) controlled closed chamber on the stage of a confocal microscope [LSM 510 (Zeiss, Welwyn Garden City, UK) or SP2 (Leica, Milton Keynes, UK)]. When appropriate, DMEM was exchanged for avian Krebs' solution. Isolated or filter-mounted retinas were positioned with the ventricular zone facing the objective.

Imaging cell movement

Labeled cells were located using epifluorescence illumination. The fluorescence of DiI was excited using the 543 nm line of the argon–krypton laser, whereas Oregon Green or eGFP was excited using the 488 nm line of the argon laser. *xy* images (in the plane of the retinal surface) were taken at 1 μm steps, throughout the depth of the retina and ~5 μm on either side. This was repeated at 30 s to 15 min intervals, depending on the experiment. Images were analyzed off-line using Zeiss LSM, Leica, or MetaMorph software. Individual *xy* scans were built into a *xyz* stack to give a three-dimensional image of the retina. Image stacks were rotated about the *x*-axis and projected to give an *xz* image series over time. Measurements of the position of cell nuclei were made relative to the ventricular surface. The center of the cell body was defined as the intersection of two diagonal lines drawn between the corners of a box fitted to the bulge containing the cell nucleus. The distance between this point and the outer edge of the ventricular zone was measured for each time point, and the speed of movement was determined.

Imaging spontaneous calcium activity

Retinas were loaded with Oregon Green BAPTA-AM (10 μM; Invitrogen) and the dispersant Cremophor-EL (0.03%; Sigma) for 1.5 h at 36°C and then maintained in gassed Krebs' solution at 36°C. Whole-mount neural retinas were transferred to the stage of an inverted microscope (LSM510; Zeiss) as described above. *xy* or *xz* (through the depth of the retina), 12-bit images were acquired at 3–15 s intervals and analyzed off-line. The mean fluorescence of individual cells was calculated and normalized to its initial value at time 0. A change in fluorescence in excess of a criterion level of 10% above baseline was accepted as an event. Spontaneous Ca^{2+} waves were defined as groups of three or more cells undergoing a spatially and temporally coordinated increase in $[Ca^{2+}]_i$ above criterion level.

To achieve the time resolution required to monitor changes in $[Ca^{2+}]_i$ during migration, it was necessary to record these cells using single confocal plane *z*-scans through the thickness of the retina. It is possible that transient changes in fluorescence intensity seen during nuclear movement are attributable to changes in the volume of the cell within the imaging plane rather than changes in $[Ca^{2+}]_i$. Ratiometric measurements were conducted to assess whether changes in Oregon Green fluorescence recorded in this way accurately represent $[Ca^{2+}]_i$ levels. Retinas were coloaded with Oregon Green and Indo-1. Indo-1 and Oregon Green were sequentially excited using the 350 nm line of the UV laser and the 488 nm line of the argon laser, respectively. Fluorescence emissions from Oregon Green and Indo-1 were recorded simultaneously at 405 ± 10 and 480 ± 10 nm, respectively. During binding, Ca^{2+} Oregon Green exhibits an increase in fluorescence, whereas the fluorescence of Indo-1 AM emission collected at 480 ± 10 nm decreases. Uniform changes in the fluorescence of both dyes are expected if the volume of a cell in the imaging plane changes or a more brightly labeled part of the cytoplasm enters the confocal plane. Simultaneous dual-emission *z*-scans of cells undergoing interkinetic nuclear movement revealed that transient increases in the fluorescence of Oregon Green were accompanied by decreases in the fluorescence of Indo-1 (supplemental Fig. 2, available at www.jneurosci.org as supplemental material). These changes shared the same onset, shape, and time course of those obtained with Oregon Green, indicating that the changes in Oregon Green fluorescence accurately reflect changes in $[Ca^{2+}]_i$.

Imaging dye-filled cells

Flat-mounted retinas were viewed on a confocal microscope. Fluorescent profiles were located using epifluorescence illumination before taking a series of *xy* optical sections, ~1 μm apart, throughout the depth of the retina. The fluorescence of FITC and Cy3 were sequentially excited using the 488 nm line of an argon laser and the 543 nm line of a helium–neon laser, respectively. Three-dimensional projections of the *xyz* stacks, generated as described above, were made and then rotated through 90° about the *x*-axis to produce an *xz* view.

Statistics

Results are presented as the mean ± SEM, *N* indicates the number of retinas investigated, and *n* indicates the number of cells recorded. SEM and *p* values were derived from a minimum of $N = 4$ retinas for each condition. The speed of interkinetic nuclear movement in the presence and absence of drugs was compared using an unpaired Student's *t* test, assuming unequal variance, unless otherwise stated, in which a one-way ANOVA test, with Dunnett's correction for multiple comparisons, was used instead.

Drugs

Carbenoxolone (100 μM), retinoic acid (RA) (25 μM), and 18-α-glycyrrhetinic acid (18-α-GA) (50 μM) were purchased from Sigma. BAPTA-AM was purchased from Invitrogen. The mimetic peptides Gap26 (VCYDKSFPISHVR) and scrambled Gap26 (PSFDSRHCIVKYV) were obtained from Severn Biotech (Worcestershire, UK). They were acetylated and amidated to mimic the peptide *in situ* within the protein. Pairs of retinas from the same embryo were used, one as control and the other was treated with the appropriate drug.

Results

Migratory behavior of embryonic retinal cells

Progenitor cell interkinetic nuclear movement is poorly understood. As a prelude to investigating factors that might influence

this process, we first sought to characterize interkinetic nuclear movements in the early embryonic retina at a time when progenitors are rapidly dividing. Progenitor cells were followed in real time, *in vivo*, using time-lapse confocal microscopy. Cells undergoing interkinetic nuclear movement had a bipolar shape (supplemental Fig. 1*B*, available at www.jneurosci.org as supplemental material), with an elongated cell body and processes extending to the ventricular and vitreal surfaces. It was not possible to distinguish between progenitor and postmitotic cells on the basis of morphology alone. However, because postmitotic cells are born in the ventricular zone and migrate away to other levels in the retina, it is generally assumed that cells moving toward the ventricular zone are progenitors in G_2 of the cell cycle (supplemental Fig. 1*B*, available at www.jneurosci.org as supplemental material). The population of cells moving away from the ventricular zone contains both progenitor cells in G_1 and postmitotic cells (G_0). Recently, newborn horizontal cells, which in the adult occupy the region immediately below the photoreceptor layer, have been shown to first move toward the immature ganglion cell layer but subsequently return to a region just below the ventricular zone (Edqvist and Hallbook, 2004). However, this behavior was only observed from E7, significantly later than the period under observation in this study (E5). The cell types born at E5 (ganglion and amacrine cells) reside at the vitreal surface of the retina and migrate directly from the ventricular zone to the vitreal side of the retina after terminal division. Thus, the population of cells moving toward the ventricular zone is predominantly composed of progenitor cells at the stage used in our experiments.

Interkinetic nuclear movement in progenitor cells

Figure 1*A* shows the nuclei of three typical DiI-labeled progenitor cells undergoing interkinetic movement, imaged over ~3 h at 15 min intervals (such movements can be more clearly seen in supplemental Movie 1, available at www.jneurosci.org as supplemental material). At the start of the recording, the nuclei of cells 1 and 3 were located approximately halfway between the ventricular and vitreal surfaces of the retina. During the recording period, the nucleus of cell 1 moved rapidly and that of cell 3 more slowly, toward the ventricular zone before dividing. The nucleus of cell 2 moved at a slower rate in the direction of the ventricular zone, moving a total of 20 μm during the period shown. Nuclear movement is characterized by phases of movement interspersed by periods in which nuclei move only slowly or are stationary (Fig. 1*A–C*). Progenitor cells only moved radially; no tangential movement was observed. On approach to the ventricular zone, the progenitor cell nuclei lost their elongated shape and rounded up (Fig. 1*A*,*D*, cells 1 and 3). Nuclei located between 20 and 80 μm from the ventricular zone had an average length/width ratio of 3.2 (range of 1.6–4.3). Those located in the ventricular zone, and up to 20 μm away, had a ratio of 1.1 ± 0.1 (range of 0.8–1.8) (data from $N = 53$ retinas, $n = 389$ cells).

Previous evidence suggested that a progenitor cell retracts its vitreal process during division (Hinds and Ruffett, 1971; Seymour and Berry, 1975; Chenn and McConnell, 1995; Fukushima et al., 2000). However, recent findings indicate that this process is retained through mitosis and inherited by one of the daughter cells (Miyata et al., 2001; Noctor et al., 2002; Saito et al., 2003). In our preparations, retention of the vitreal contact throughout cell division was frequently, but not always, observed. In the example shown in Figure 1*A*, cell 1 retained its contact with the vitreal surface throughout mitosis (arrowheads), and the two daughter cells remained in close physical contact after mitosis. However, on a number of occasions, we observed the clear retraction of the vitreal process as the nucleus entered the ventricular zone (Fig. 1*E*), suggesting that the maintenance of contact with the vitreal surface may not be an absolute requirement for division. The role of the vitreal process in cell division warrants additional investigation.

Interkinetic nuclear movements are not linear (Fig. 1*A–D*). Images were acquired at a frequency of 0.05 Hz for shorter periods of time to examine the dynamics of interkinetic nuclear movement in detail. At this more rapid sampling frequency, the movements of progenitor cell nuclei were composed of frequent short stationary phases that alternated with periods of movement in a forward or backward direction. An example of this movement is shown in Figure 1, *F* and *G*. During a period of ~18 min, the nucleus moved in a stepwise manner toward the ventricular zone; it spent a total of 12 min making movements in this direction, interspersed with opposite movements (a total of 2 min 40 s) and periods during which it remained stationary (totaling 3 min).

The movements of nuclei moving toward the vitreal surface were very similar to those of cells moving in the opposite direction. The cell shown in Figure 1*H* was typical of the population of cells moving in the vitreal direction. At the start of the recording, the nucleus was located in the ventricular half of the retina, 25 μm away from the ventricular zone. During the period of observation, the nucleus made saltatory movements toward the vitreal surface (Fig. 1*I*,*J*), acquiring a more elongated bipolar shape as it went (Fig. 1*K*). As with cells moving toward the ventricular zone, only radial, and no tangential, movements were observed.

Speed of nuclear translocation during interkinetic nuclear movement

At E5, the average speed of interkinetic nuclear movement was 20.7 ± 0.5 μm/h ($N = 53$, $n = 389$). The speed of movement of nuclei moving toward the ventricular zone (progenitor cells in G_2) was 20.5 ± 0.7 μm/h (range of 2.5–68.6 μm/h; $N = 53$, $n = 213$) (Fig. 2*A*), whereas those moving in the vitreal direction (mixed population of progenitor cells and postmitotic cells) did so at 21.0 ± 0.8 μm/h (range of 4.5–64.2 μm/h; $N = 53$, $n = 176$) (Fig. 2*B*). The number of proliferative divisions is high at E5 but, because neurons are also born at this time (Prada et al., 1991; Snow and Robson, 1994), the population of cells moving away from the ventricular zone likely includes postmitotic cells. Chenn and McConnell (1995) proposed that, in the cortex, these two populations migrate at different speeds, with immature neurons migrating at velocities ~10-fold greater than progenitor cells. However, the distribution of velocities for the population of retinal cells moving away from the ventricular zone is almost identical to that seen for the population moving toward it; both are unimodal with a single peak at 16–20 μm/h (Fig. 2*A*,*B*), and median values of 19.1 and 18.5 μm/h, respectively. Because there was no statistical difference between the mean speeds of interkinetic nuclear movement in cells moving toward or away from the ventricular zone ($p = 0.617$, Student's t test), migratory velocities are presented as the mean of the two populations (cells moving toward and away from the ventricular zone) in the remaining figures; the separate speeds for the two populations are given in the text and figure legends.

Ca^{2+} transients are associated with movement

The migration of postmitotic cells requires a change in $[Ca^{2+}]_i$ (Komuro and Rakic, 1996, 1998). Spontaneous Ca^{2+} transients are also a common feature of progenitor cells (Owens and Krieg-

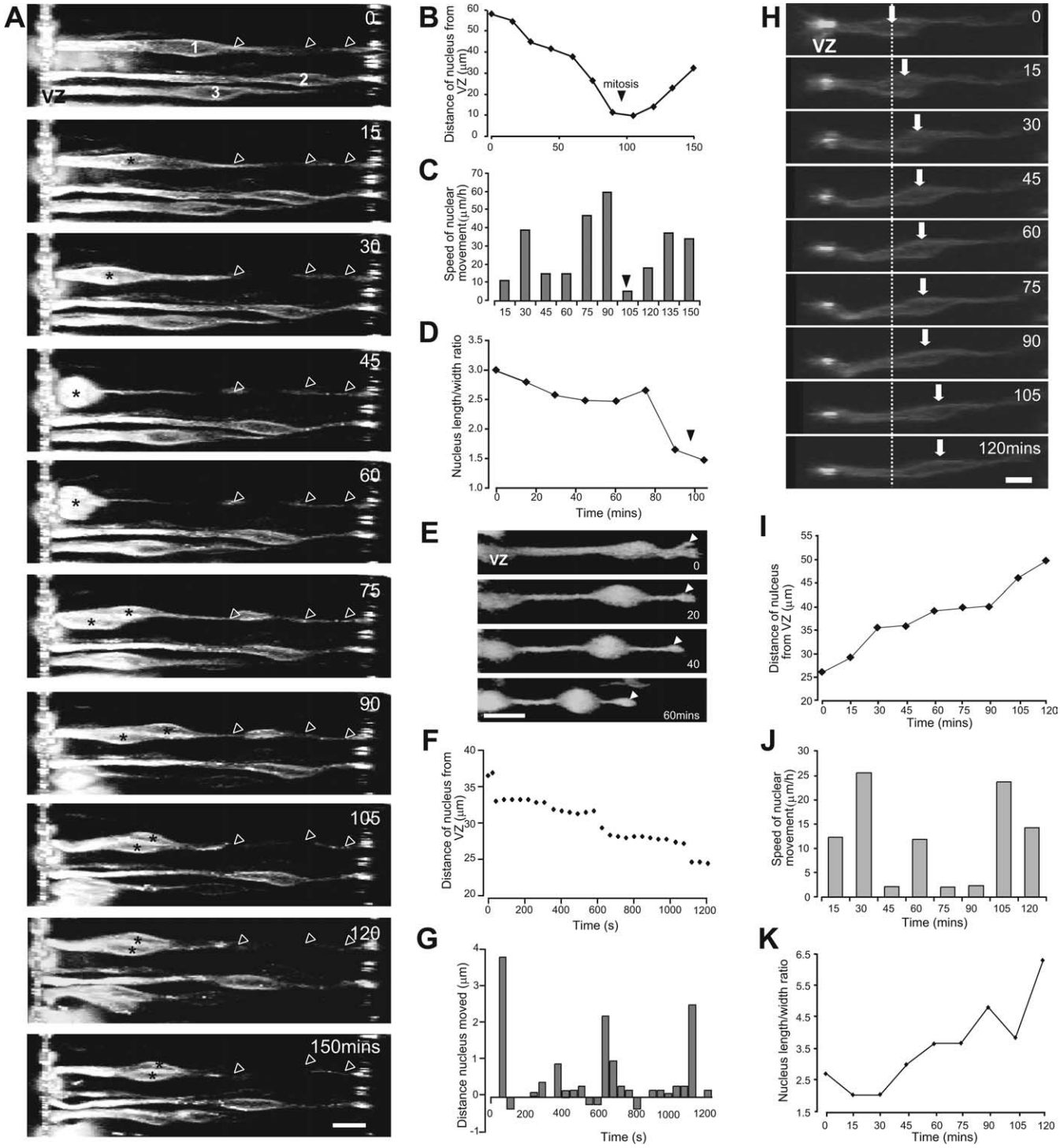

Figure 1. Interkinetic nuclear movement in the retina. ***A***, Time-lapse image sequence of progenitor cell nuclei moving toward the ventricular zone (supplemental Movie 1, available at www.jneurosci.org as supplemental material). Three cells are shown (1–3). The nuclei of cells 1 and 3 made saltatory movements toward the ventricular zone. The cell bodies rounded up before division. Cell 1 retains its contact with the vitreal surface throughout division (arrowheads). After division, the daughter cells remain in close contact as they move away from the ventricular zone (asterisks, cell 1). ***B–D***, Details of the movements of cell 3. The distance traveled (***B***), the speed of nuclear movement (***C***), and the length/width ratio of the cell body (***D***) are each shown as a function of time. Mitosis occurs between 90 and 105 min. After this time, measurements are shown for the daughter cell nearest the ventricular zone. ***E***, Example of a progenitor cell that retracts the vitreal process (arrowhead) as it migrates toward the ventricular zone. ***F***, ***G***, Interkinetic nuclear movement is saltatory in progenitor cells moving toward the ventricular zone. ***F***, The distance traveled by a nucleus moving toward the ventricular zone as a function of time. Images were acquired at 40 s intervals. ***G***, Histogram of the distance moved by the nucleus in each 40 s period. Positive values represent movement toward the ventricular zone, and negative values represent a movement toward the putative ganglion cell layer. ***H–K***, The behavior of cells undergoing interkinetic nuclear movements toward the vitreal surface was very similar to that of cells moving toward the ventricular zone. ***H***, Time-lapse sequence of a progenitor cell nucleus moving away from the ventricular zone (supplementary Movie 1, available at www.jneurosci.org as supplemental material). The positions of the nucleus at time 0 (dashed line) and at each time point (arrow) are marked. The cell body elongates as it moves away from the ventricular zone. The distance traveled (***I***), the speed of movement (***J***), and the length/width ratio of the cell body (***K***) are each shown as a function of time. Scale bars, 10 μm.

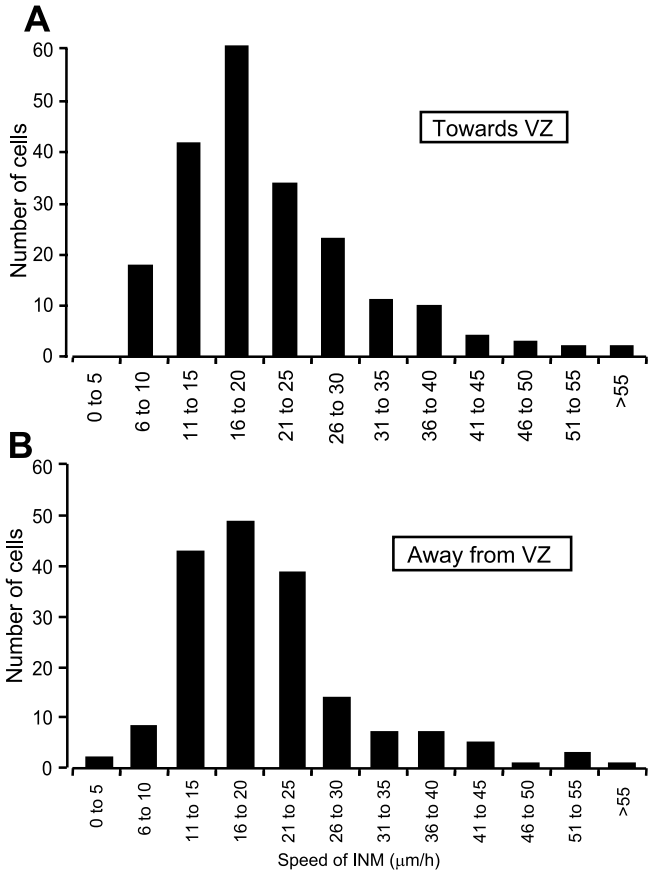

Figure 2. Speeds of interkinetic nuclear movement (INM) toward and away from the ventricular zone (VZ). The individual rates for cell nuclei moving toward (***A***) and away (***B***) from the ventricular zone were sorted into 5 μm/h bins.

stein, 1998; Pearson et al., 2002, 2004). Here we provide evidence to suggest that spontaneous Ca^{2+} transients are involved in the translocation of progenitor cell nuclei. Cells labeled with the Ca^{2+} indicator Oregon Green moved in a saltatory manner, at a speed of 22 ± 3 μm/h ($N = 10$, $n = 14$), indicating that labeling with Oregon Green did not impair interkinetic nuclear movement. Transient changes in $[Ca^{2+}]_i$ often preceded a period of nuclear movement (see Materials and Methods) (supplemental Fig. 2, available at www.jneurosci.org as supplemental material). Figure 3*A–D* shows examples of such Ca^{2+} transients; in each case, the cells underwent an increase in $[Ca^{2+}]_i$ just before a phase of nuclear movement. Of the cells showing Ca^{2+} transients, 78% made nuclear movements immediately after the Ca^{2+} transient ($N = 17$, $n = 23$). Only 13% of cell nuclei moved in the absence of a measurable change in $[Ca^{2+}]_i$ (Fig. 3*E*). These transients were observed in cells undergoing nuclear movement both toward and away from the ventricular zone. Buffering changes in $[Ca^{2+}]_i$ by incubation with BAPTA-AM (100 μM) greatly reduced the speed of nuclear movement (Fig. 3*F*). In paired controls, cells underwent interkinetic nuclear movement at a speed of 21 ± 2 μm/h ($N = 4$, $n = 32$); this was reduced by 81%, to 4 ± 1 μm/h in cells preincubated in BAPTA-AM ($N = 4$, $n = 30$; $p < 0.01$, Student's t test). The findings described here indicate that spontaneous $[Ca^{2+}]_i$ transients precede movements of the nucleus and that inhibiting these transients significantly impairs translocation of the nucleus during interkinetic nuclear movement.

Gap junctions modulate interkinetic nuclear movement

Gap-junctional communication has been demonstrated to modulate the rate of migration of a number of immature cell types (Ewart et al., 1997; Huang et al., 1998; Bannerman et al., 2000) and proliferation in the embryonic retina (Becker and Mobbs, 1999). Retinal progenitor cells form gap junction-coupled networks that primarily exclude differentiated cells (Pearson et al., 2004), and gap junction-dependent Ca^{2+} waves occur that reflect this pattern of coupling (Fig. 4*A*,*B*) (Pearson et al., 2004). It is possible that gap junction-mediated signals, such as Ca^{2+} waves, represent a mechanism for neighboring cells to coordinate events within the cell cycle and/or interkinetic nuclear movement (Pearson et al., 2004; Weissman et al., 2004). DiI labeling provides circumstantial evidence for coordinated movements; dye particles labeled groups of neighboring cells, and cell nuclei within these clusters were frequently observed to move in synchrony (Fig. 4*C*). Here, we examined the effects of changing intercellular communication via gap-junction channels on progenitor cell interkinetic nuclear movement.

Interkinetic nuclear movement is slowed by gap-junction blockers

We used a panel of pharmacological gap-junction channel blockers (CBX, 100 μM; 18-α-GA, 50 μM; and RA, 25 μM) to examine the influence of gap-junction coupling on interkinetic nuclear movement. Application of each of the three blockers used significantly impaired interkinetic nuclear movement (Fig. 5*A*,*B*). Application of CBX reduced the average speed of migration by 56%, from 15 ± 2 μm/h ($N = 6$, $n = 94$) in controls to 8 ± 1 μm/h ($N = 6$, $n = 63$) ($p < 0.01$, Student's t test). The populations moving toward and away from the ventricular zone were similarly affected (control, toward 15 ± 1 μm/h and away 14 ± 1 μm/h; CBX, toward 6 ± 1 μm/h and away 8 ± 1 μm/h). Application of 18-α-GA slowed movement by 66%, from 19 ± 2 μm/h ($N = 6$, $n = 62$) in controls to 8 ± 1 μm/h ($N = 6$, $n = 58$) ($p < 0.01$, Student's t test), and both the toward and away populations were similarly affected (control, toward 21 ± 2 μm/h and away 19 ± 1 μm/h; 18-α-GA, toward 7 ± 1 μm/h and away 5 ± 2 μm/h). Similar, but less marked, effects were seen after application of RA; cell nuclei moved at 21 ± 2 μm/h ($N = 5$, $n = 46$) in controls and 10 ± 1 μm/h ($N = 5$, $n = 48$) in the presence of RA, a reduction of 47% ($p < 0.01$, Student's t test). Again, both the toward and away populations were similarly affected (control, toward 22 ± 2 μm/h and away 19 ± 1 μm/h; RA toward 11 ± 2 μm/h and away 9 ± 1 μm/h). The uniform effect of the panel of gap-junction blockers used makes it unlikely that these were attributable to any nonspecific actions of these drugs. Thus, pharmacological blockade of gap junctions significantly impairs progenitor cell interkinetic nuclear movement.

Interfering with gap-junction channel formation slows interkinetic nuclear movement

Cx43 is likely to mediate the gap-junction coupling seen between retinal progenitors in early development (Becker et al., 2002; Pearson et al., 2004). Therefore, electroporation of a pIRES2 vector with a cytomegalovirus promoter were used to express eGFP and dnCx43, eGFP and wild-type Cx43, or eGFP alone (Becker et al., 2001). Control eGFP cell nuclei made saltatory movements at an average of 12 ± 1 μm/h ($N = 5$, $n = 60$) (Fig. 5*C*,*D*) and moved at similar speeds both toward (13 ± 2 μm/h) and away (9 ± 1 μm/h) from the ventricular zone. The average speed of interkinetic nuclear movement recorded in eGFP preparations

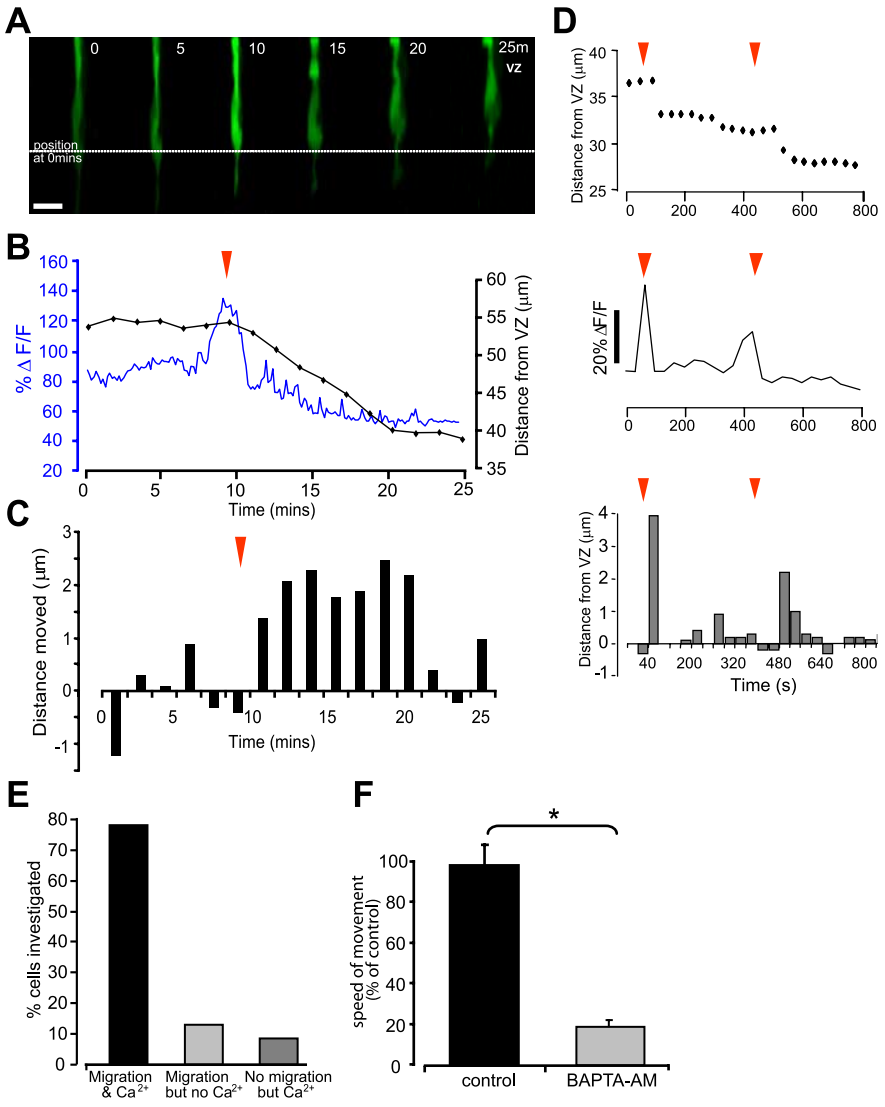

Figure 3. Ca^{2+} transients and cell movement. ***A***, Single confocal images from a time series of a progenitor cell labeled with Oregon Green–dextran. The cell undergoes a transient change in $[Ca^{2+}]_i$ before moving toward the ventricular zone. Scale bar, 10 μm. ***B***, Trace showing changes in $[Ca^{2+}]_i$ (blue) in the soma of the cell shown in ***A*** as $\Delta F/F$ and the position of the nucleus relative to the ventricular zone (black). ***C***, Histogram of the distance moved by the nucleus in each time period. Positive values represent movement toward the ventricular zone, and negative values represent a movement toward the vitreal surface. For *p* values, see Results. ***D***, Second example of Ca^{2+} transients preceding nucleus translocation. Position of the nucleus relative to the ventricular zone (top) and changes in $[Ca^{2+}]_i$ as $\Delta F/F$ as a function of time (middle). Two transients occurred during the imaged period (red arrows). Bottom, Histogram of the distance moved by the cell in each time period. ***E***, Histogram showing the correlation between movement and preceding Ca^{2+} transients. ***F***, Nuclear movement requires a change in $[Ca^{2+}]_i$. Histogram showing the effects of the Ca^{2+} chelator BAPTA on the speed of interkinetic nuclear movement. $^*p < 0.01$, Student's *t* test.

was slower than in those labeled with DiI (see above), probably as a result of the extended incubation period required for GFP expression (overnight vs acute dissection). The rate of interkinetic nuclear movement was reduced by 64% in cells transfected with the dnCx43 construct to 4 ± 1 μm/h ($N = 5$, $n = 96$; $p < 0.01$, ANOVA with Dunnett's correction) (Fig. 5*C*,*D*). The average rate of movement toward the ventricular zone was 6 ± 1 μm/h ($n = 55$) compared with 2 ± 1 μm/h away from the ventricular zone ($n = 41$). Cells transfected with the wild-type Cx43 construct showed interkinetic nuclear movement at speeds faster than eGFP controls, although the effect was not statistically significant (15 ± 1 μm/h; $N = 3$, $n = 33$; $p = 0.085$, ANOVA with Dunnett's correction) (Fig. 5*C*,*D*). Here, cell nuclei moved at similar speeds both toward (16 ± 3 μm/h) and away (15 ± 2 μm/h) from the ventricular zone.

The dnCx43 construct interferes with gap-junction channel formation and, because of the high degree of homology between different connexins, potentially affects other connexins. However, Cx43 protein expression can be transiently and specifically knocked down by antisense oligodeoxynucleotides (Becker and Mobbs, 1999; Becker et al., 1999; McGonnell et al., 2001), providing an alternative technique by which to test the specific role of Cx43 in interkinetic nuclear movement. Furthermore, whereas pIRES dnCx43 constructs only affect communication in the eGFP-expressing transfected cells, application of Cx43 antisense specifically reduces expression of Cx43 protein in the whole tissue (Fig. 5*G*). Application of Cx43 asODNs caused a 52% reduction in the speed of interkinetic nuclear movement. Control cells treated with pluronic gel (the vehicle for the ODN) alone showed interkinetic nuclear movement at an average of 12 ± 1 μm/h ($N = 4$, $n = 49$; toward 12 ± 1 μm/h and away 11 ± 1 μm/h) (Fig. 5*E*,*F*), whereas cell nuclei in antisense-treated retinas moved at an average of 5 ± 1 μm/h ($N = 4$, $n = 48$; $p < 0.02$, Student's *t* test). Nuclear movements toward (6 ± 1 μm/h) and away (4 ± 1 μm/h) from the ventricular zone were similarly affected by the asODNs.

Gap-junction hemichannels modulate interkinetic nuclear movement

Cells may communicate via gap junctions directly linking the cytoplasm of two neighboring cells or indirectly by the release of substances through unopposed connexons, known as hemichannels. There is increasing evidence for hemichannel signaling in a variety of systems, including the generation of Ca^{2+} waves (Bennett et al., 2003; Weissman et al., 2004; Pearson et al., 2005). Here, we investigated the presence of hemichannels in the embryonic neural retina and examined their potential role in the regulation of interkinetic nuclear movement.

Hemichannels in the neural retina

To determine whether gap-junction hemichannels are present in the embryonic neural retina, we used an antibody (Gap7M) that binds to a region on the first external loop of the connexin, which is only exposed on unopposed gap-junction hemichannels and so does not bind to complete gap junctions (Becker et al., 1995; Pearson et al., 2005). Labeling revealed sparse punctate immunoreactivity distributed throughout the neural retina (Fig. 6*A*, arrows). Staining was absent from controls in which the primary antibody was omitted (Fig. 6*B*).

The pharmacological and molecular tools used above to block whole gap-junction channels also act at unopposed gap-junction

hemichannels. Therefore, we used a connexin mimetic peptide, Gap26, to examine the specific role of hemichannels in interkinetic nuclear movement. Gap26 blocks hemichannels by mimicking a 13 amino acid sequence (VCYDKSFPISHVR) on the first extracellular loop. A study on endothelial cell lines found Gap26 to act on hemichannels alone, without affecting coupled gap junctions (Braet et al., 2003). We have demonstrated recently Gap26 to be similarly specific for hemichannels in the embryonic chick retinal pigment epithelium (Pearson et al., 2005). Here, dye-fill experiments (described by Pearson et al., 2004) were used to assess the specificity of Gap26 for hemichannels in the neural retina. Retinal progenitor cells are extensively coupled via gap junctions, as demonstrated by the spread of the tracer Neurobiotin from an injected cell to its neighbors (Fig. 6*C*) (Pearson et al., 2004). This spread is blocked by the gap-junction blocker CBX (Fig. 6*E*). Conversely, preincubation with Gap26 for the same duration as used in the migration experiments described below (2 h) had no effect on dye coupling (Fig. 6*D*). Thus, when used in this manner, Gap26, unlike CBX, acts on unopposed hemichannels but not whole gap junctions (for additional proof of specificity, see Pearson et al., 2005).

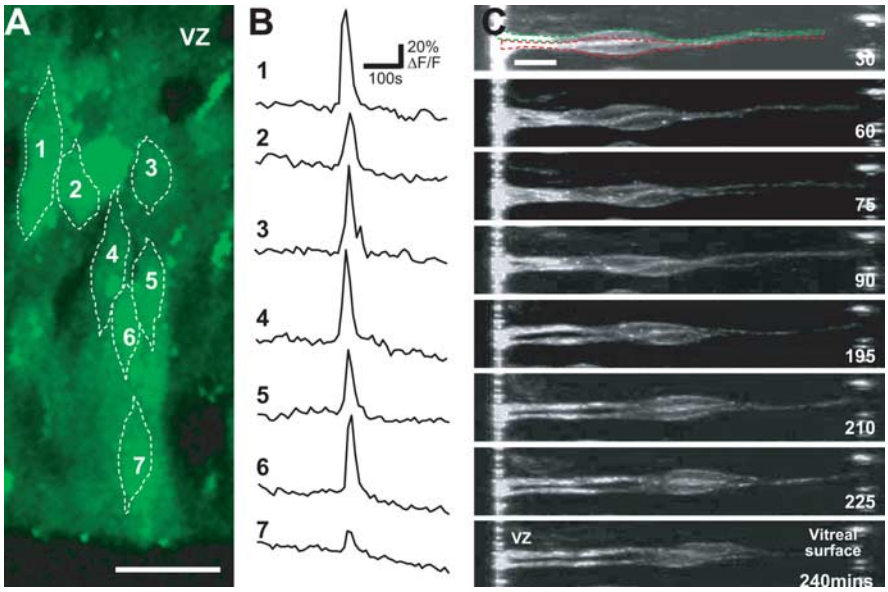

Figure 4. Coordinated Ca^{2+} transients and interkinetic nuclear movement. ***A***, Confocal image of a section through the thickness of the neural retina from a time series showing a column of cells undergoing a spontaneous coordinated $[Ca^{2+}]_i$ wave. VZ, Ventricular zone. ***B***, Traces showing fluorescence changes in cells 1–7 depicted in the image. ***C***, Adjacent cells show synchronous nuclear movements. Images from a time series showing adjacent cell nuclei moving toward the vitreal surface. Individual cells are outlined in the first image. Scale bars, 10 μm.

After incubation in Gap26 (0.25 mg/ml), the speed of interkinetic nuclear movement was reduced by 28% (Fig. 6*F*,*G*). Control cells incubated in a scrambled version of the peptide (0.25 mg/ml) showed interkinetic nuclear movements at an average of 18 ± 1 μm/h ($N = 4$, $n = 99$), whereas those incubated in Gap26 moved at the slightly, but significantly, slower speed of 13 ± 1 μm/h ($N = 4$, $n = 95$; $p < 0.01$, Student's t test). The effect of Gap26 in slowing the movements of nuclei moving toward the ventricular zone was more marked (20 ± 1 μm/h in scrambled peptide; 14 ± 1 μm/h in Gap26; $p < 0.01$, Student's t test) than for those moving away (14 ± 1 μm/h in scrambled peptide; 13 ± 1 μm/h in Gap26; $p = 0.067$, Student's t test). The reasons for this difference are unclear.

Discussion

Interkinetic nuclear movement is an essential part of the progenitor cell cycle (Murciano et al., 2002), yet little is known about such movements or the mechanisms that might regulate them. Here, using real-time imaging, we provide the first characterization of progenitor cell interkinetic nuclear movement in the retina and present evidence to demonstrate a hitherto unknown role of gap-junctional communication and Ca^{2+} signaling in the regulation of these movements. Progenitor cell nuclear movement is saltatory and associated with Ca^{2+} transients that can spread between these cells as waves. Furthermore, gap junctions are required for nuclei to move at their normal rate. The reduction in the speed of interkinetic nuclear movement caused by gap-junction blockade provides a potential explanation for the decrease in proliferation that also results from impaired gap-junctional communication, as described in previous studies (Becker and Mobbs, 1999); a reduced speed of nuclear movement will decrease the rate at which progenitor cell nuclei arrive in the ventricular zone, the only region in which they can undergo cell division (Roberts et al., 1985).

Properties of interkinetic nuclear migration in the retina

Retinal cells undergoing interkinetic nuclear movement display characteristic changes in morphology. Progenitor cells are of bipolar shape with an elongated cell body and processes that project to either side of the retina. Time-lapse imaging experiments reveal that the cell nucleus translocates within these processes and that the cell body rounds up on approach to the ventricular zone, elongating again during exit. Such behavior is similar to that seen in previous anatomical studies of progenitor cell cycling (Sauer, 1935; Sidman et al., 1959; Seymour and Berry, 1975; Nagele and Lee, 1979). In the retina, interkinetic nuclear movement is characterized by the frequent alternation of periods of forward movement with phases in which the cell nucleus is stationary. Furthermore, translocation of the nucleus requires a change in $[Ca^{2+}]_i$; spontaneous Ca^{2+} transients were temporally correlated with periods of nuclear movement, and chelation of $[Ca^{2+}]_i$ with BAPTA prevented these movements. Such saltatory, Ca^{2+}-dependent movements are reminiscent of those seen in migrating postmitotic neurons (Komuro and Rakic, 1996; Nadarajah et al., 2001), suggesting that similar mechanisms may be involved in these two processes.

The speed of interkinetic nuclear movement in the retina was similar for nuclei moving toward and away from the ventricular zone (~21 μm/h) and of the same magnitude as that reported for cortical progenitor cells (~18 μm/h) (Chenn and McConnell, 1995). However, Chenn and McConnell proposed that progenitor cells and immature neurons move away from the ventricular zone at widely different speeds. They found that the two progenitor daughter cells resulting from a symmetric division moved away from the ventricular zone at like rates and at a speed much slower than that seen during G_2. Conversely, they report that,

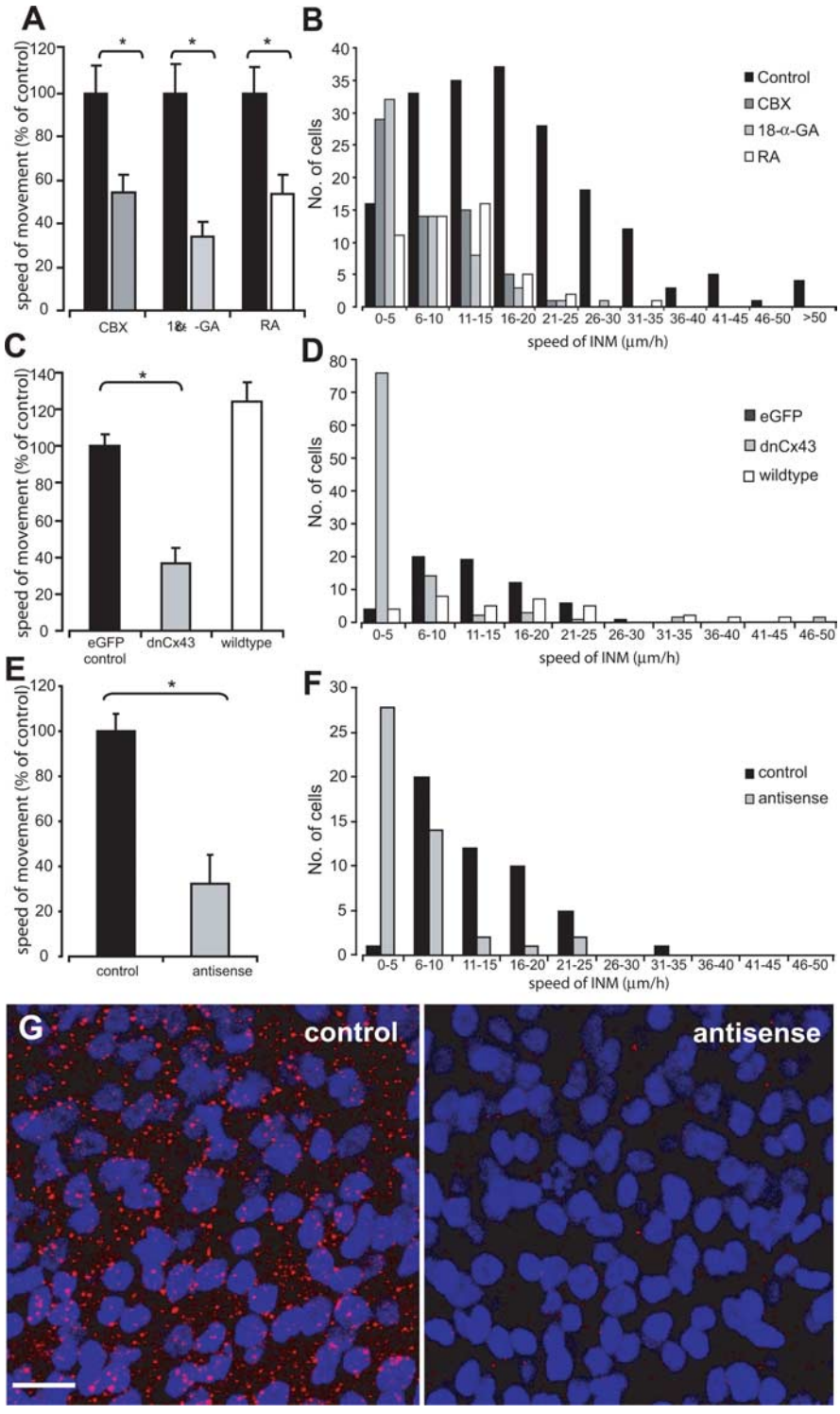

Figure 5. The effects of gap-junction blockers on interkinetic nuclear movement. ***A***, Graph showing the effects of CBX (100 μM), 18-α-GA (50 μM), and RA (25 μM) compared with controls (black bars) on the average speed of interkinetic nuclear movement. *$p < 0.01$, Student's *t* test. ***B***, Distribution of interkinetic nuclear movement speeds in controls and in the presence of the different gap-junction blockers. ***C***, Graph showing the effects of dnCx43 and wild-type Cx43 on the average speed of interkinetic nuclear movement. *$p < 0.01$, ANOVA with Dunnett's correction. ***D***, Distribution of interkinetic nuclear movement speeds in controls and in cells transfected with either dnCx43 or wild-type Cx43. ***E***, Graph showing the effects of Cx43 asODNs on the average speed of interkinetic nuclear movement in all cells. *$p < 0.02$, Student's *t* test. ***F***, Distribution of interkinetic nuclear movement speeds in controls and after topical application of Cx43 asODNs. ***G***, Cx43 staining (red) in controls (left) and after application of Cx43 asODNs (right). The preparations were counterstained with Hoechst 33342 (blue) to label the nuclei. Images are projections of 10 confocal sections taken at 1 μm steps through the ventricular zone of each retinal preparation. For additional details of the extent of connexin knockdown, see Materials and Methods. Scale bar, 10 μm.

after an asymmetric division, which produces one postmitotic and one progenitor cell, the progenitor cell moves away slowly (~1 μm/h), whereas the postmitotic daughter moves at a rate 10-fold faster. In contrast, we find that, in the retina, the population of cells moving away from the ventricular zone moves at the same rate as progenitor cells moving toward it. Despite there being significant levels of neurogenesis at the time studied (Prada et al., 1991; Snow and Robson, 1994), there was no evidence to suggest that there is one group that moves faster than another. The same wide range of velocities of interkinetic nuclear movement was observed for both the progenitor population (moving toward the ventricular zone) and the mixed population of progenitor and postmitotic cells (moving away from the ventricular zone).

Postmitotic cells can undergo both radial and tangential dispersion (Fekete et al., 1994; O'Rourke et al., 1997; Komuro et al., 2001), but whether progenitor cells undergo tangential dispersion is unclear. Reid et al. (1995) suggested that cortical progenitor cells moved through the ventricular zone, pausing periodically to generate subclones. However, we found that, in the retina, all movements of cells occurred within the radial plane with no evidence of tangential migration, suggesting that tangential dispersion occurs after postmitotic cells reach the layer appropriate to their fate. This notion is supported by studies of transgenic mosaic mouse retinas, in which tangential migration was found to be a property of postmitotic cells (Reese and Tan, 1998).

Gap junctions modulate interkinetic nuclear movement

In the retina, the ventricular zone (the equivalent of the outer region of the ventricular zone in the cortex) is the only location in which cells can divide. Thus, it is possible that factors that regulate the proliferative cycle could do so by modulating the rate at which cells undergo interkinetic nuclear movement and therefore reach a region permissive for cell division. Mathematical models have demonstrated the need for interkinetic nuclear movement in maintaining proliferation (Murciano et al., 2002) based on evidence that local cell–cell interactions and lateral inhibition by Notch and Delta are important in determining whether cells remain proliferative or differentiate (Henrique et al., 1995; Lewis, 1998). When interkinetic nuclear movement was excluded from a model of proliferation/neurogenesis, an

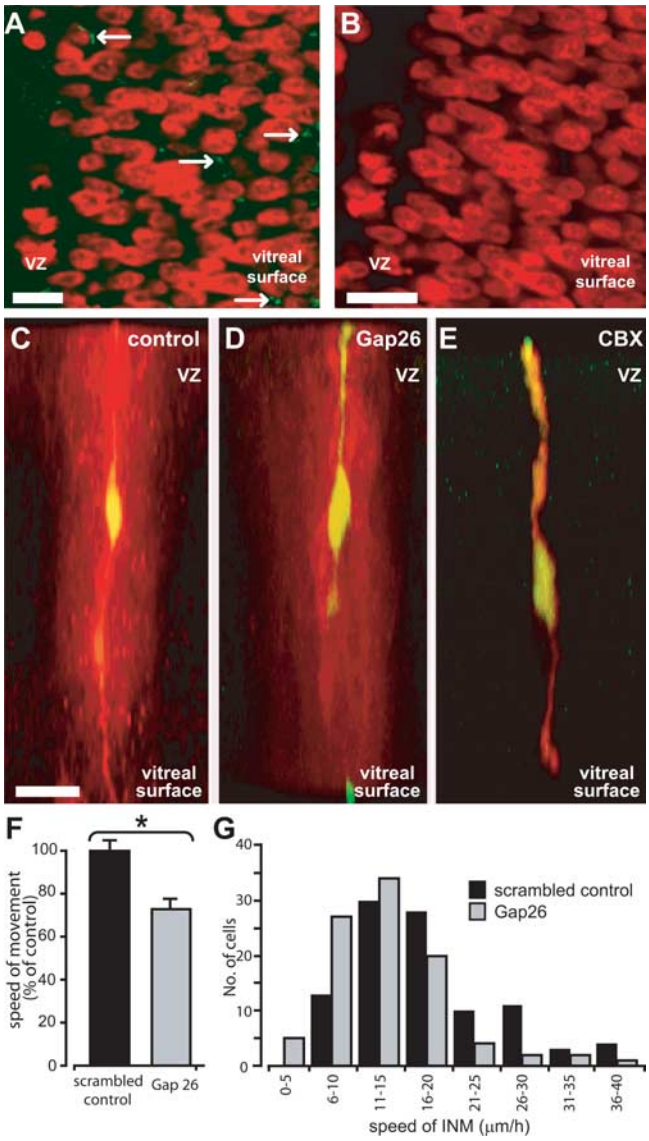

Figure 6. The effects of hemichannel blockers on interkinetic nuclear movement. ***A***, High-power projection of five confocal sections taken at 1 μm intervals of a retina that has been labeled with Hoechst 33342 (pseudocolored red) and Alexa 488-tagged Gap7M (green), which labels connexin hemichannels. Sparse punctate staining is seen throughout the neural retina (arrows). VZ, Ventricular zone. ***B***, Control staining in which the primary antibody was omitted. ***C–E***, Dye fills confirm the specificity of Gap26 for gap-junction hemichannels. Cells in the neural retina filled with the gap junction-impermeant marker FITC–dextran and the gap junction-permeant tracer Neurobiotin (appears yellow when colocalized) are dye coupled to a large number of adjacent cells (red) in controls (***C***). Coupling is prevented by CBX (***E***) but not by Gap26 (***D***). Scale bars, 10 μm. ***F***, Graph showing the effects of the hemichannel blocker Gap26 and scrambled peptide on the average speed of interkinetic nuclear movement. *$p < 0.01$, Student's *t* test. ***G***, Distribution of speeds of interkinetic nuclear movement (INM) after incubation with Gap26 and in scrambled control. Scale bars: ***A***, ***B***, 5 μm; ***C–E***, 10 μm.

enhanced rate of neurogenesis was predicted attributable to a greater physical interaction between proliferating and differentiating cells.

The factors that modulate interkinetic nuclear migration are poorly understood. Here, using a variety of pharmacological and molecular tools, we demonstrate for the first time that gap-junctional communication is essential for the maintenance of normal progenitor cell interkinetic nuclear movement. Gap-junction coupling is a common feature of progenitor cells (LoTurco and Kriegstein, 1991; Bittman et al., 1997; Becker et al., 2002; Pearson et al., 2004) and is an essential requirement for maintaining cultures of mouse neural stem cells in a proliferative state (Cheng et al., 2004). Furthermore, suppressing the expression of Cx43, which here we have shown to slow interkinetic nuclear movement, leads to a reduction in progenitor cell proliferation and produces small eyes (Becker and Mobbs, 1999). In keeping with these findings, short-term pharmacological block of interkinetic nuclear movement leads to an initial overproduction of retinal ganglion cells (Murciano et al., 2002), suggesting that downregulation of coupling promotes neurogenesis. Thus, it would appear that one way in which gap junctions might act to promote proliferation is via their actions on progenitor cell nuclear movements.

How might gap-junction function promote nuclear movement? Here, we have shown that Ca^{2+} transients are required to drive nuclear translocation during interkinetic nuclear movement. Similar Ca^{2+} transients spread to neighboring cells in the form of gap junction-dependent waves (this paper and Pearson et al., 2004). One possible explanation for the positive actions of gap-junction coupling on interkinetic nuclear movement is that coupled cells experience a higher frequency of Ca^{2+} transients, attributable to those spreading from neighboring cells, than uncoupled cells would. Work on immature neurons has shown that the speed of their migration is positively correlated with the frequency of Ca^{2+} transients (Komuro and Rakic, 1996). Thus, an increased frequency of Ca^{2+} transients may lead to an increase in the number of translocating movements made by the nucleus and hence the speed of interkinetic nuclear migration overall (supplemental Fig. 3, available at www.jneurosci.org as supplemental material).

Because gap-junctional communication provides a means by which local groups of progenitor cells can exchange developmentally relevant signals, coupling could facilitate synchronized entry into the different phases of the cell cycle. Many of the cells that form coupled clusters in the ventricular zone are clonally related (Cai et al., 1997b; Reese and Tan, 1998). The variation in cell cycle times between cortical progenitor cells of the same age is minimal (Cai et al., 1997a); clonal descendents progress through the cell cycle in synchrony and form tight clusters (Cai et al., 1997a,b). We frequently observed adjacent retinal progenitor cells moving in apparent synchrony with one another. Gap junctions may thus act to locally coordinate the cell cycle via interkinetic nuclear movement; Ca^{2+} waves passing between progenitor cells via this route may represent one such synchronizing signal. More controversially, it is possible, given that the mimetic peptide Gap26 causes some slowing of movement, that hemichannels also play a similar role in synchronizing the movements and division of retinal progenitor cells. Weissman et al. (2004) have shown that, in the rodent cortical ventricular zone, Ca^{2+} signals can be initiated by release of the neurotransmitter ATP and that hemichannels may be involved in the release mechanism. Given that retinal progenitor cells express purinergic P2Y receptors and that ATP leads to a change in $[Ca^{2+}]_i$ (Pearson et al., 2002), the modulation of interkinetic nuclear movement by hemichannels reported here may also involve hemichannel-mediated ATP release. Furthermore, Manent et al. (2005) have demonstrated recently that the rate of neuronal migration is modulated by neurotransmitters released via a nonvesicular mechanism. Here, we show that the specific inhibition of gap-junction hemichannels in the retina slows interkinetic nuclear movement, suggesting that the effects described after pharmacological and molecular manipulation of

gap-junction function may arise from the combined effects on both whole gap junctions and hemichannels.

The mechanisms that regulate interkinetic nuclear movement are central to understanding the cell cycle in both normal and abnormal development and to developing strategies that use stem or retinal progenitor cells in therapeutic interventions. Here, we have examined interkinetic nuclear movement in retinal progenitor cells and present evidence for a previously unappreciated role for gap junctions in its regulation. Additional experiments are required to elucidate the precise role of the Ca^{2+} signals that pass between retinal progenitor cells via gap junctions, together with the role of hemichannels, in the control of progenitor cell movement and proliferation in the retina.

References

Bannerman P, Nichols W, Puhalla S, Oliver T, Berman M, Pleasure D (2000) Early migratory rat neural crest cells express functional gap junctions: evidence that neural crest cell survival requires gap junction function. J Neurosci Res 61:605–615.

Becker DL, Mobbs P (1999) Connexin alpha1 and cell proliferation in the developing chick retina. Exp Neurol 156:326–332.

Becker DL, Evans WH, Green CR, Warner A (1995) Functional analysis of amino acid sequences in connexin43 involved in intercellular communication through gap junctions. J Cell Sci 108:1455–1467.

Becker DL, McGonnell I, Makarenkova H, Patel K, Tickle C, Lorimer J, Green CR (1999) Roles for alpha 1 connexin in morphogenesis of chick embryos using a novel antisense approach. Dev Genet 24:33–42.

Becker DL, Ciantar D, Catsicas M, Pearson R, Mobbs P (2001) Use of pIRES vectors to express EGFP and connexin constructs in studies of the role of gap junctional communication in the early development of the chick retina and brain. Cell Commun Adhes 8:355–359.

Becker DL, Bonness V, Catsicas M, Mobbs P (2002) Changing patterns of ganglion cell coupling during chick retinal development. J Neurobiol 52:280–293.

Bennett MV, Contreras JE, Bukauskas FF, Saez JC (2003) New roles for astrocytes: gap junction hemichannels have something to communicate. Trends Neurosci 26:610–617.

Bittman K, Owens D, Kriegstein A, LoTurco J (1997) Cell coupling and uncoupling in the ventricular zone of the developing neocortex. J Neurosci 17:7037–7044.

Braet K, Vandamme W, Martin PE, Evans WH, Leybaert L (2003) Photoliberating inositol-1,4,5-trisphosphate triggers ATP release that is blocked by the connexin mimetic peptide gap 26. Cell Calcium 33:37–48.

Cai L, Hayes NL, Nowakowski RS (1997a) Local homogeneity of cell cycle length in developing mouse cortex. J Neurosci 17:2079–2087.

Cai L, Hayes NL, Nowakowski RS (1997b) Synchrony of clonal cell proliferation and contiguity of clonally related cells: production of mosaicism in the ventricular zone of developing mouse neocortex. J Neurosci 17:2088–2100.

Catsicas M, Bonness V, Becker D, Mobbs P (1998) Spontaneous Ca^{2+} transients and their transmission in the developing chick retina. Curr Biol 8:283–286.

Cheng A, Tang H, Chai J, Zhu M, Zhang X, Rao M, Mattson M (2004) Gap junctional communication is required to maintain mouse cortical neural progenitor cells in a proliferative state. Dev Biol 272:203–216.

Chenn A, McConnell SK (1995) Cleavage orientation and the asymmetric inheritance of Notch1 immunoreactivity in mammalian neurogenesis. Cell 82:631–641.

Edqvist PH, Hallbook F (2004) Newborn horizontal cells migrate bidirectionally across the neuroepithelium during retinal development. Development 131:1343–1351.

Ewart JL, Cohen MF, Meyer RA, Huang GY, Wessels A, Gourdie RG, Chin AJ, Park SM, Lazatin BO, Villabon S, Lo CW (1997) Heart and neural tube defects in transgenic mice overexpressing the Cx43 gap junction gene. Development 124:1281–1292.

Fekete DM, Perez-Miguelsanz J, Ryder EF, Cepko CL (1994) Clonal analysis in the chicken retina reveals tangential dispersion of clonally related cells. Dev Biol 166:666–682.

Fukushima N, Weiner JA, Chun J (2000) Lysophosphatidic acid (LPA) is a novel extracellular regulator of cortical neuroblast morphology. Dev Biol 228:6–18.

Gan WB, Grutzendler J, Wong WT, Wong RO, Lichtman JW (2000) Multicolor "DiOlistic" labeling of the nervous system using lipophilic dye combinations. Neuron 27:219–225.

Henrique D, Adam J, Myat A, Chitnis A, Lewis J, Ish-Horowicz D (1995) Expression of a Delta homologue in prospective neurons in the chick. Nature 375:787–790.

Hinds JW, Ruffett TL (1971) Cell proliferation in the neural tube: an electron microscopic and golgi analysis in the mouse cerebral vesicle. Z Zellforsch Mikrosk Anat 115:226–264.

Honig MG, Hume RI (1986) Fluorescent carbocyanine dyes allow living neurons of identified origin to be studied in long term cultures. J Cell Biol 103:171–187.

Huang GY, Cooper ES, Waldo K, Kirby ML, Gilula NB, Lo CW (1998) Gap junction-mediated cell-cell communication modulates mouse neural crest migration. J Cell Biol 143:1725–1734.

Komuro H, Rakic P (1996) Intracellular Ca^{2+} fluctuations modulate the rate of neuronal migration. Neuron 17:275–285.

Komuro H, Rakic P (1998) Orchestration of neuronal migration by activity of ion channels, neurotransmitter receptors, and intracellular Ca^{2+} fluctuations. J Neurobiol 37:110–130.

Komuro H, Yacubova E, Yacubova E, Rakic P (2001) Mode and tempo of tangential cell migration in the cerebellar external granule layer. J Neurosci 21:527–540.

Lewis J (1998) Notch signalling and the control of cell fate choices in vertebrates. Semin Cell Dev Biol 9:583–589.

LoTurco JJ, Kriegstein AR (1991) Clusters of coupled neuroblasts in embryonic neocortex. Science 252:563–566.

Lumsden A, Sprawson N, Graham A (1991) Segmental origin and migration of neural crest cells in the hindbrain region of the chick embryo. Development 113:1281–1291.

Manent JB, Demarque M, Jorquera I, Pellegrino C, Ben-Ari Y, Aniksztejn L, Represa A (2005) A noncanonical release of GABA and glutamate modulates neuronal migration. J Neurosci 25:4755–4765.

McGonnell IM, Green CR, Tickle C, Becker DL (2001) Connexin43 gap junction protein plays an essential role in morphogenesis of the embryonic chick face. Dev Dyn 222:420–438.

Miyata T, Kawaguchi A, Okano H, Ogawa M (2001) Asymmetric inheritance of radial glial fibers by cortical neurons. Neuron 31:727–741.

Murciano A, Zamora J, Lopez-Sanchez J, Frade JM (2002) Nuclear interkinetic movement may provide spatial clues to the regulation of neurogenesis. Mol Cell Neurosci 21:285–300.

Nadarajah B, Brunstrom J, Grutzendler J, Wong ROL, Pearlman AL (2001) Two modes of radial migration in early development of the cerebral cortex. Nat Neurosci 4:143–150.

Nagele RG, Lee HY (1979) Ultrastructural changes in cells associated with interkinetic nuclear migration in the developing chick neuroepithelium. J Exp Zool 210:89–106.

Noctor SC, Flint AC, Weissman TA, Wong WS, Clinton BK, Kriegstein AR (2002) Dividing precursor cells of the embryonic cortical ventricular zone have morphological and molecular characteristics of radial glia. J Neurosci 22:3161–3173.

O'Rourke NA, Chenn A, McConnell SK (1997) Postmitotic neurons migrate tangentially in the cortical ventricular zone. Development 124:997–1005.

Owens DF, Kriegstein AR (1998) Patterns of intracellular calcium fluctuation in precursor cells of the neocortical ventricular zone. J Neurosci 18:5374–5388.

Pearson R, Catsicas M, Becker DL, Mobbs P (2002) Purinergic and muscarinic modulation of the cell cycle and Ca^{2+} signalling in the chick retinal ventricular zone. J Neurosci 22:7569–7579.

Pearson RA, Catsicas M, Becker DL, Bayley P, Luneborg NL, Mobbs P (2004) Ca^{2+} signaling and gap junction coupling within and between pigment epithelium and neural retina in the developing chick. Eur J Neurosci 19:2435–2445.

Pearson RA, Dale N, Llaudet E, Mobbs P (2005) ATP released via gap junction hemichannels from the pigment epithelium regulates neural retinal progenitor proliferation. Neuron 46:731–744.

Prada C, Puga J, Perez-Mendez L, Lopez R, Ramirez G (1991) Spatial and temporal patterns of neurogenesis in the chick retina. Eur J Neurosci 3:559–569.

Reese BE, Tan SS (1998) Clonal boundary analysis in the developing retina

using X-inactivation transgenic mosaic mice. Semin Cell Dev Biol 9:285–292.

Reid CB, Liang I, Walsh C (1995) Systematic widespread clonal organization in cerebral cortex. Neuron 15:299–310.

Robinson SR, Rapaport DH, Stone J (1985) Cell division in the developing cat retina occurs in two zones. Brain Res 351:101–109.

Saito K, Kawaguchi A, Kashiwagi S, Yasugi S, Ogawa M, Miyata T (2003) Morphological asymmetry in dividing retinal progenitor cells. Dev Growth Differ 45:219–229.

Sauer FC (1935) Mitosis in the neural tube. J Comp Neurol 62:377–405.

Seymour RM, Berry M (1975) Scanning and transmission electron microscope studies of interkinetic nuclear migration in the cerebral vesicles of the rat. J Comp Neurol 160:105–125.

Sidman RL, Miale IL, Feder N (1959) Cell proliferation and migration in the primitive ependymal zone: an autoradiographic study of histogenesis in the nervous system. Exp Neurol 1:322–333.

Snow RL, Robson JA (1994) Ganglion cell neurogenesis, migration and early differentiation in the chick retina. Neuroscience 58:399–409.

Tamalu F, Chiba C, Saito T (2001) Gap junctional coupling between progenitor cells at the retinal margin of adult goldfish. J Neurobiol 48:204–214.

Weissman TA, Riquelme PA, Ivic L, Flint AC, Kriegstein AR (2004) Calcium waves propagate through radial glial cells and modulate proliferation in the developing neocortex. Neuron 43:647–661.

Wright CS, Becker DL, Lin JS, Warner AE, Hardy K (2001) Stage-specific and differential expression of gap junctions in the mouse ovary: connexin-specific roles in follicular regulation. Reproduction 121:77–88.